ELSEVIER

Journal of Molecular Catalysis A: Chemical 141 (1999) 205–214

JOURNAL OF MOLECULAR CATALYSIS A: CHEMICAL

Mechanistic study of the hydrogen exchange and hydrogenation of propene over alumina supported rhodium and ruthenium carbonyl cluster complexes

Shuichi Naito [a,*], Mitsutoshi Tanimoto [b]

[a] *Department of Applied Chemistry, Faculty of Engineering, Kanagawa University, 3-27-1, Rokkakubashi, Kanagawa-ku, Yokohama 221, Japan*

[b] *Department of Chemistry, Faculty of Science, Shizuoka University, 864, Ohoya, Shizuoka, Japan*

Abstract

The mechanism of propene–deuterium reaction over alumina-supported Rh and Ru carbonyl cluster complexes was studied with kinetic investigation as well as microwave spectroscopic analysis of monodeuteropropene. Irrespective of the nuclearity and the kind of metals, similar catalytic behavior was observed in both C_3H_6–C_3D_6 and C_3H_6–D_2 reactions over $Rh_4(CO)_{12}/Al_2O_3$, $Rh_6(CO)_{16}/Al_2O_3$ and $Ru_3(CO)_{12}/Al_2O_3$, suggesting the formation of common surface complexes as $[M(CO)_2]_n$ by impregnation. Different catalytic behavior of fixed carbonyl cluster complexes from that over freshly reduced metal surface (Rh/Al_2O_3) and CO preadsorbed metal surface($CO/Rh/Al_2O_3$), suggests the existence of an unique catalytically active species such as metal–metal bridged hydrides for the hydrogen exchange process of propene molecules.

Keywords: Mechanism; Propene–deuterium reaction; Rh and Ru carbonyl cluster complexes

1. Introduction

The interaction of metal carbonyl cluster complexes with inorganic metal oxide surfaces has been extensively investigated because of the possibility to prepare structure-controllable catalysts, having new activity and selectivity. Their structural changes by supporting have been recognized by many surface techniques, and several different surface structures have been reported. Among them, $Rh_4(CO)_{12}$ [1], $Rh_6(CO)_{16}$ [2] and $Ru_3(CO)_{12}$ [3–5] complexes on alumina were the most thoroughly clarified systems, and common surface complexes as $[M(CO)_2X_2]_n$ were proposed. The catalytic behavior of these surface complexes seems to be very interesting in analogy with that of CO preadsorbed metal surfaces. However, only few catalytic reactions have been studied on these fixed catalysts such as hydrogenation of CO [6–8], investigating the correlation of the catalytic activity and selectivity change with the structure of the active sites.

Microwave spectroscopy is a powerful technique for the study of hydrogen exchange or isomerization reaction of propene or butene [9]. It enables us to determine the hyperfine distribution of the D atoms in the exchanged d_1-mole-

* Corresponding author.

1381-1169/99/$ - see front matter
PII: S1381-1169(98)00264-7

cule. The location of the D atoms in the products reveals the previous points of attachment of the adsorbed molecules to the catalysts. Consequently, it is a good probe reaction for the investigation of the correlation between the structure of reaction intermediates and the active sites. We have applied this technique to investigate the structure sensitivity of supported metal [10–12] and metal oxide [13,14] catalysts and demonstrated its validity as a prove reaction.

In the present study, we investigated the mechanism of the hydrogen exchange reaction of propene (C_3H_6–D_2 and C_3H_6–C_3D_6 reaction) over $Rh_4(CO)_{12}/Al_2O_3$, $Rh_6(CO)_{16}/Al_2O_3$, and $Ru_3(CO)_{12}/Al_2O_3$ catalysts. We applied microwave spectroscopy to analyze the deuterated position in propene molecules, from which we could determine the reaction intermediates in the hydrogen exchange process. The correlation between the surface structure and the reaction intermediates is discussed in detail, and a unique exchange mechanism common to these fixed catalysts is proposed.

2. Experimental

2.1. Catalyst preparation

Alumina support (Aerosil Aluminum Oxide C) was evacuated at 723 K for two hours, and kept under nitrogen atmosphere. Metal carbonyl cluster complexes, $Rh_4(CO)_{12}$, $Rh_6(CO)_{16}$ and $Ru_3(CO)_{12}$ (purchased from Strem Chemicals) were dissolved in a dry *n*-hexane solution under vacuum and then mixed with the pretreated alumina to form slurry under vacuum and stirred vigorously for 24 h. The amount of CO liberated during this procedure was measured by gas chromatography. The slurry was freed from the solvent by vacuum distillation, and 1 wt.% of metal concentration catalysts were prepared.

2.2. Infrared spectra

Samples for ir measurements were prepared by the same procedure as mentioned above except that an alumina disk (20 mm diameter, ca 50 mg) was used as a support, which was evacuated at 723 K before impregnation. The disk thus prepared was inserted in an ir cell equipped with KBr windows under nitrogen. The cell was connected to a closed gas circulation system and various pretreatments were carried out before ir measurements. Fourier transform infrared spectra were recorded by a JEOL JIR-DIAMOND 20 spectrometer with the resolution of 2 cm^{-1} (512 scans).

2.3. Reaction procedure

Trace amounts of oxygen in H_2 and D_2 gases from commercial cylinder were removed by circulating the gases over a heated palladium black catalyst. C_3H_6 and C_3D_6 were purchased from Takachiho Kagaku KK and from Merck, Sharp and Dohme, respectively. They were purified by a freeze–thaw cycle. $CHD{=}CH{-}CH_3$ was prepared from 1-bromoprop-1-ene according to a procedure described in the literature [15].

The reaction was carried out in a closed gas circulation system (total volume 350 cm^3). The supported catalyst (0.5 g) was put into the reaction vessel under nitrogen, which was connected to the circulation system, and evacuated for 20 h at room temperature (base pressure 10^{-3} Pa). Then the catalyst was cooled to the reaction temperature under vacuum, and the mixed reaction gases (C_3H_6–D_2 or C_3H_6–C_3D_6) were introduced to start the reaction. Before each run, the catalysts were evacuated for 3 h at room temperature.

2.4. Detection methods: mass spectrometry and microwave spectroscopy

A small amount (a few percent) of the reaction gas was sampled at certain intervals during

the reaction and separated into propane and propene by gas chromatography (alumina column, He carrier). The deuterium contents in propene were determined with a mass spectrometer (Hitachi RMU-6MG), using ionization voltage of 15 eV. The location of the deuterium atom in monodeuteropropene was determined by recording the microwave absorption lines (1_{01}–0_{00} rotational transitions) characteristic of each isotopic species. The detailed procedures were reported previously. The isotopic isomers in monodeuteropropene are as follows;

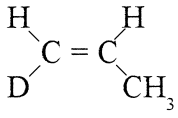

c-1-d_1

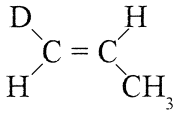

t-1-d_1

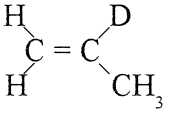

2-d_1

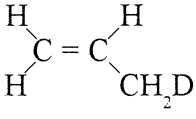

3-d_1

3. Results

3.1. Identification of the fixed surface species

It is well known that Rh and Ru carbonyl cluster complexes easily react with surface OH groups of alumina support under evacuation, to form $[M(CO)_2X_2]_n$ type surface complexes, where X is the oxygen atom of alumina. The amount of liberated CO during 24 h of impregnation procedure was about 3–4 molecules per one metal carbonyl cluster complex in the cases of $Rh_4(CO)_{12}$ and $Rh_6(CO)_{16}$, and five molecules in the case of $Ru_3(CO)_{12}$, suggesting the formation of such surface complexes as $M(CO)_2$. Fig. 1 summarizes the infrared spectra

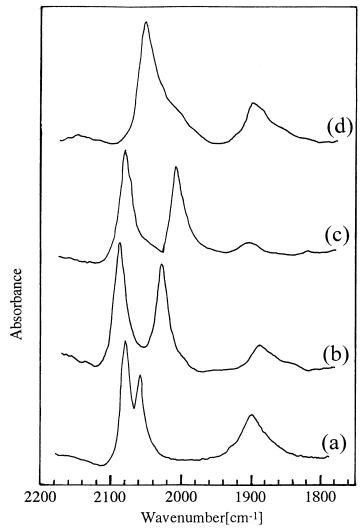

Fig. 1. Infrared spectra of fixed carbonyl cluster complexes. (a) $Rh_4(CO)_{12}/Al_2O_3$. (b) $Rh_6(CO)_{16}/Al_2O_3$. (c) $Ru_3(CO)_{12}/Al_2O_3$. (d) CO adsorption on Rh/Al_2O_3.

of fixed carbonyl cluster complexes, where two intense bands were observed at 2090–2060 and 2030–2000 cm^{-1} regions, assignable to $[M(CO)_2X_2]_n$ surface complexes. These complexes are quite stable at room temperature and no spectra changes were observed after C_3H_6–D_2 and C_3H_6–C_3D_6 reactions at lower temperatures. Alumina supported Rh and Ru metal catalysts were prepared by the reduction of $Rh_4(CO)_{12}/Al_2O_3$ and $Ru_3(CO)_{12}/Al_2O_3$, respectively, by hydrogen at 723 K. Metal dispersions of the reduced catalysts were determined by hydrogen adsorption at room temperature; $Rh/Al_2O_3 = 78\%$, $Ru/Al_2O_3 = 67\%$. The infrared spectra of adsorbed CO on Rh/Al_2O_3 is also shown in the figure, which is different from $[Rh(CO)_2X_2]_n$ surface complexes.

3.2. C_3H_6–C_3D_6 and C_3H_6–D_2 reactions over $Rh_4(CO)_{12}/Al_2O_3$

When equimolar amounts of C_3H_6 and C_3D_6 (15 Torr each) were introduced onto $Rh_4(CO)_{12}/Al_2O_3$ at 245 K, both C_3H_5D and C_3HD_5 were formed at the initial stage of the

reaction through the dissociative adsorption of propene molecules (C_3H_5(a)) as shown in Scheme 1(a) or associative adsorption (C_3H_6D(a)) if there is an available surface deuteride as shown in Scheme 1(c). Fig. 2(a) demonstrates the microwave spectroscopic analyses of the deuterium distribution in monodeuteropropene formed in this hydrogen exchange process. At the initial stage of the reaction, *c*- and *t*-propene-1-d_1 (38% each) as well as propene-2-d_1 (24%) are the main products. The amount of propene-3-d_1 is almost 0% at the initial stage, but increased considerably as the reaction proceeded, accompanied with the decrease of propene 1-d_1. This distribution change with time indicates the presence of the intramolecular 1,3-hydrogen shift process [10] (Scheme 1(d)) during intermolecular hydrogen exchange of propene. To confirm this intramolecular process, only propene-1-d_1 was introduced onto the catalyst. The propene-3-d_1 increased with the decrease of propene-1-d_1 similar to Fig. 2. The dotted line in Fig. 2(a) represents the isotopic distribution in the C_3H_6–C_3D_6–D_2 (1:1:2) reaction. Hydrogen exchange of propene took place with the same rate as the case of C_3H_6–C_3D_6 reaction together

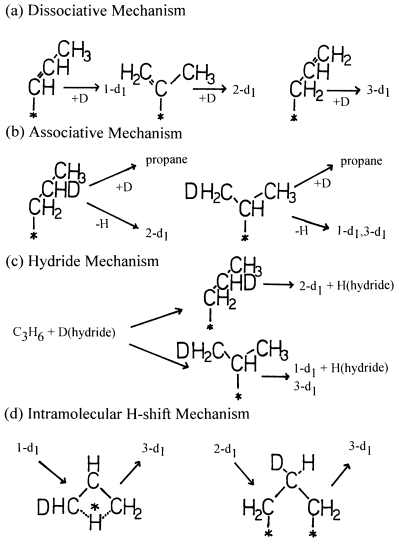

Scheme 1. Possible reaction scheme and intermediates of propene–deuterium reaction.

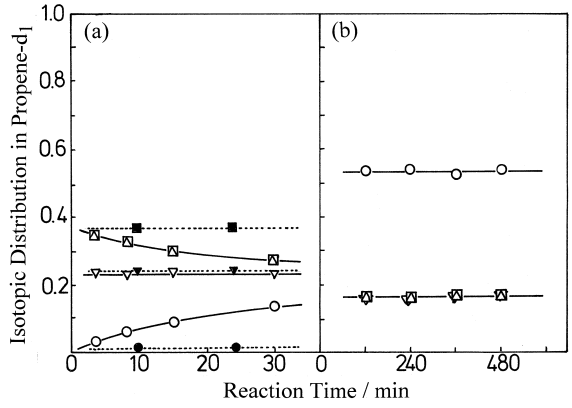

Fig. 2. Time courses of the isotopic distribution in propene-d_1 during the reactions. (a) C_3H_6–C_3D_6 (open symbols) and C_3H_6–C_3D_6–D_2 (closed symbols) at 245 K and (b) C_3H_6–D_2 at 273 K over $Rh_4(CO)_{12}/Al_2O_3$. P(propene) = 15 Torr, $P(D_2)$ = 30 Torr. 0.5 g of catalyst. □ ■, *c*-1-d_1; △ ▲, *t*-1-d_1; ▽ ▼, 2-d_1; ○ ●, 3-d_1.

with much slower formation of propane, but no intramolecular 1,3-hydrogen shift was observed. This result suggests that gaseous hydrogen blocks the reaction site for intramolecular hydrogen shift reaction.

The isotopic distribution pattern in Fig. 2(a) depends on reaction temperatures, and the proportion of propene-2-d_1 was increased at lower reaction temperature. Fig. 3 summarizes the temperature dependence of the initial exchange rate (TOF of each propene-d_1 isomer formation)

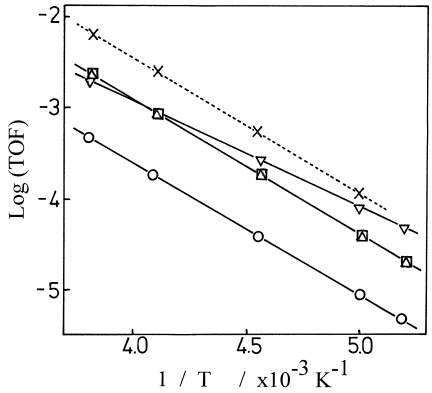

Fig. 3. Temperature dependence of the TOF of each propene-d_1 isomer in C_3H_6–C_3D_6 reaction (solid line) and HD formation in H_2–D_2 reaction (dotted line) over $Rh_4(CO)_{12}/Al_2O_3$. P(propene) = 15 Torr, and P(hydrogen) = 30 Torr. 0.5 g of catalyst. □, *c*-1-d_1; △, *t*-1-d_1; ▽, 2-d_1; ○, 3-d_1; ×, HD.

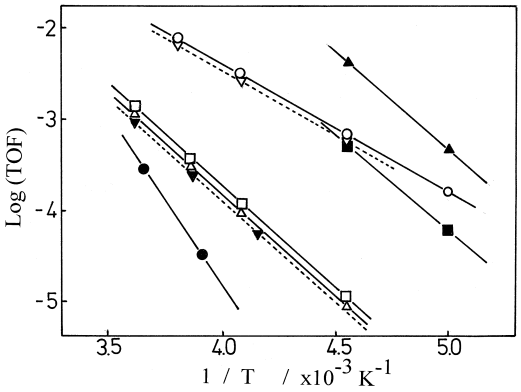

Fig. 4. Temperature dependence of the TOFs of C_3H_6–C_3D_6 and C_3H_6–D_2 reactions over $Rh_4(CO)_{12}/Al_2O_3$ (open symbol) and Rh/Al_2O_3 (closed symbol). P(propene) = 15 Torr, and $P(D_2)$ = 30 Torr. 0.5 g of catalyst. ○●, Initial rates of propene-d_1 formation in C_3H_6–C_3D_6 reaction; △ ▲, initial rates of propane formation in C_3H_6–D_2 reaction; □ ■, initial rates of propene-d_1 formation in C_3H_6–D_2 reaction; dotted lines represent the initial rate of HD formation in H_2–D_2 reaction with (▼) and without (▽) propene over $Rh_4(CO)_{12}/Al_2O_3$.

of each hydrogen in propene molecules. Apparent activation energy of each product was estimated from the slope of these plots as follows: $E(1\text{-}d_1) = 28.0$ kJ/mol $E(2\text{-}d_1) = 22.6$ kJ/mol and $E(3\text{-}d_1) = 27.2$ kJ/mol. The dotted line in Fig. 3 represents the HD formation rate in H_2–D_2 exchange reaction over the same $Rh_4(CO)_{12}/Al_2O_3$ catalyst, which indicates that the exchange of H–H bond in hydrogen molecules and the exchange of C–H bond in propene molecules exhibit similar TOF and activation energies.

When a mixture of D_2 (30 Torr) and C_3H_6 (15 Torr) was introduced onto $Rh_4(CO)_{12}/Al_2O_3$ at 245 K, both propane and monodeuteropropene were formed at the similar rates, through deuterium addition and exchange processes. The Arrhenius plots of these processes are summarized in Fig. 4, together with those of C_3H_6–C_3D_6 reaction mentioned above. The deuterium exchange rates in C_3H_6–D_2 reaction was nearly one order of magnitude slower than the rate of C_3H_6–C_3D_6 exchange reaction, with higher activation energy (43.1 kJ/mol). This result suggests that both addition and exchange processes in C_3H_6–D_2 reaction proceed through the same associative reaction intermediates (propyl adsorbed species) as shown in Scheme 1(b). Fig. 2(b) demonstrates the isotopic distribution pattern of the monodeuteropropene formed in the exchange process of C_3H_6–D_2 reaction. It did not show any changes with time and the product ratios were as follows: propene-3-d_1 = 53%, *c*- and *t*-propene-1-d_1 = propene-2-d_1 = 16%. This pattern indicates that all the hydrogen in propene molecules are in exchange equilibrium. The most reasonable explanation of these phenomena is that the rate determining step of C_3H_6–D_2 reaction is the dissociation of deuterium molecules. And once deuterium atom is produced on the surface by dissociation, monodeuteropropene is mainly formed through the C_3H_6–C_3D_6 reaction with much faster rate than the reverse process of propyl intermediate, which causes the equilibration of isotopic pattern in monodeuteropropene.

3.3. C_3H_6–C_3D_6 and C_3H_6–D_2 reactions over $Rh_6(CO)_{16}/Al_2O_3$ and $Ru_4(CO)_{12}/Al_2O_3$

Fig. 5 represents the temperature dependencies of C_3H_6–C_3D_6 and C_3H_6–D_2 reactions over $Rh_6(CO)_{16}/Al_2O_3$ catalyst. The trend is quite similar to the case of $Rh_4(CO)_{12}/Al_2O_3$,

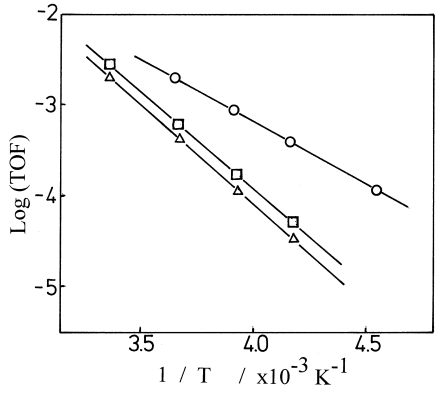

Fig. 5. Temperature dependence of the TOFs of C_3H_6–C_3D_6 and C_3H_6–D_2 reactions over $Rh_6(CO)_{16}/Al_2O_3$. P(propene) = 15 Torr, and $P(D_2)$ = 30 Torr. 0.5 g of catalyst. ○, Initial rate of propene-d_1 formation in C_3H_6–C_3D_6 reaction; △, initial rate of propane formation in C_3H_6–D_2 reaction; □, initial rate of propene-d_1 formation in C_3H_6–D_2 reaction.

although the TOF for the former catalysts were slightly smaller than the latter. The rate of monodeuteropropene formation in C_3H_6–C_3D_6 reaction was again nearly one order of magnitude faster than that in C_3H_6–D_2 reaction with smaller activation energy as follows: $E(C_3H_6$–$C_3D_6) = 28.0$ kJ/mol, and $E(C_3H_6$–$D_2) = 40.1$ kJ/mol. The time courses of the isotopic distribution patterns of monodeuteropropene in C_3H_6–C_3D_6 and C_3H_6–D_2 reactions at 260 K are shown in Fig. 6(a) and (b). The main products in the former reaction were *c*- and *t*-propene-1-d_1 (38% each) and propene-2-d_1 (24%), which are exactly the same as the case of $Rh_4(CO)_{12}/Al_2O_3$. The intramolecular hydrogen shift process again caused the increase of propene-3-d_1 with the decrease of propene-1-d_1. The isotopic distribution of monodeuteropropene formed in the latter reaction exhibited the equilibrium composition (propene-3-d_1 = 53%, *c*- and *t*-propene-1-d_1 = propene-2-d_1 = 16%). These results also suggest that the rate determining step of this reaction is the dissociation of deuterium molecules.

Fig. 7 represents the Arrhenius plots of C_3H_6–C_3D_6 and C_3H_6–D_2 reactions over $Ru_3(CO)_{12}/Al_2O_3$ catalyst. The rate of monodeuteropropene formation in the former reaction is nearly two orders of magnitudes faster than the hydrogen exchange process in the latter reaction, and the situation is the same as the case of Rh carbonyl cluster complexes. But the rate of propane formation is much smaller than that of monodeuteropropene formation in C_3H_6–D_2 reaction, which is rather different from the case of Rh cluster complexes.

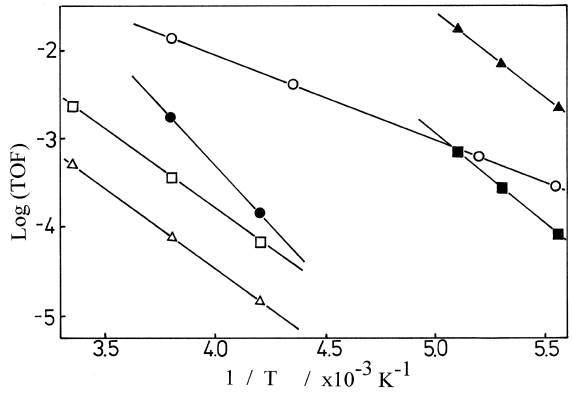

Fig. 7. Temperature dependence of the TOFs of C_3H_6–C_3D_6 and C_3H_6–D_2 reactions over $Ru_3(CO)_{12}/Al_2O_3$ (open symbol) and Ru/Al_2O_3 (closed symbol). P(propene) = 15 Torr, and $P(D_2)$ = 30 Torr. 0.5 g of catalyst. ○●, Initial rates of propene-d_1 formation in C_3H_6–C_3D_6 reaction; △▲, initial rates of propane formation in C_3H_6–D_2 reaction; □■, initial rates of propene-d_1 formation in C_3H_6–D_2 reaction.

Fig. 8(a) and (b) demonstrates the microwave spectroscopic results of isotopic distribution of

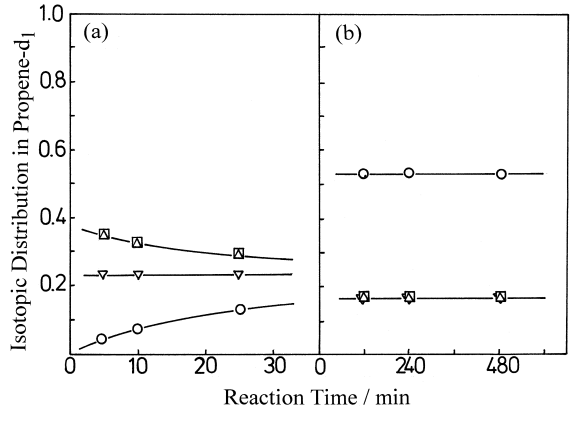

Fig. 6. Time courses of the isotopic distribution in propene-d_1 during the reaction (a) C_3H_6–C_3D_6 and (b) C_3H_6–D_2 at 260 K over $Rh_6(CO)_{16}/Al_2O_3$. P(propene) = 15 Torr, and $P(D_2)$ = 30 Torr. 0.5 g of catalyst. □, *c*-1-d_1; △, *t*-1-d_1; ▽, 2-d_1; ○, 3-d_1.

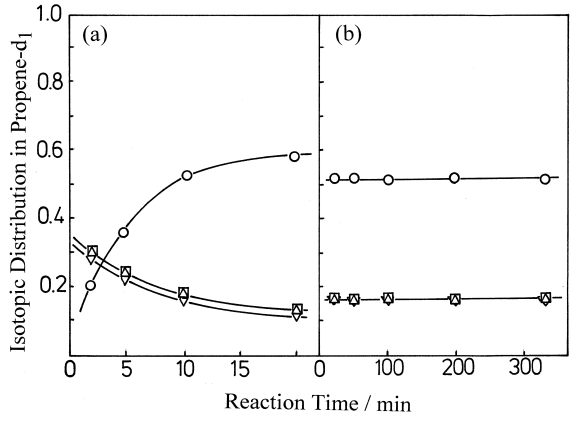

Fig. 8. Time courses of the isotopic distribution in propene-d_1 during the reaction (a) C_3H_6–C_3D_6 at 253 K and (b) C_3H_6–D_2 at 260 K over $Ru_3(CO)_{12}/Al_2O_3$. P(propene) = 15 Torr, and $P(D_2)$ = 30 Torr. 0.5 g of catalyst. □, *c*-1-d_1; △, *t*-1-d_1; ▽, 2-d_1; ○, 3-d_1.

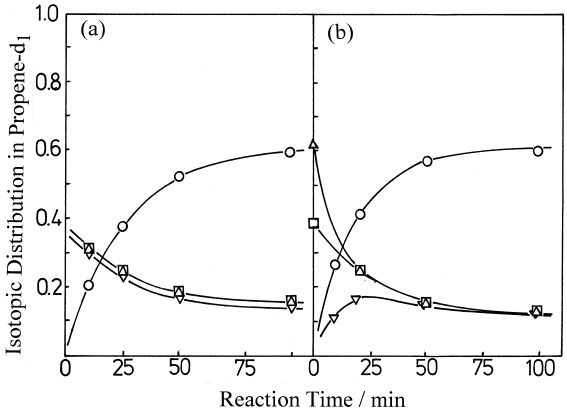

Fig. 9. Time courses of the isotopic distribution in propene-d_1 during the reaction (a) C_3H_6–C_3D_6–D_2 and (b) propene-1-d_1 + H_2 at 253 Kover $Ru_3(CO)_{12}/Al_2O_3$. P(propene) = 15 Torr, and $P(D_2)$ = 30 Torr. 0.5 g of catalyst. □, c-1-d_1; △, t-1-d_1; ▽, 2-d_1; ○, 3-d_1.

monodeuteropropene formed in both C_3H_6–C_3D_6 and C_3H_6–D_2 reactions over $Ru_3(CO)_{12}/Al_2O_3$ at 253 K and 260 K, respectively. At the initial stage of C_3H_6–C_3D_6 reaction, the main products were c- and t-propene-1-d_1 (34% each) and propene-2-d_1 (32%), which decreases considerably accompanied with the increase of propene-3-d_1. These changes indicate that intramolecular 1,3- and 2,3-hydrogen shift occurred in addition of intermolecular hydrogen exchange process. On the other hand, exchange equilibrium pattern was again obtained in the exchange process in the C_3H_6–D_2 reaction at 260 K. The isotopic distribution pattern in C_3H_6–C_3D_6–D_2 (1:1:2) reaction at 253 K was shown in Fig. 9(a), where hydrogen exchange took place with the same rate as the case of C_3H_6–C_3D_6 reaction, but intramolecular hydrogen shift process was retarded in one forth by the presence of gaseous hydrogen. This result again indicates that gaseous hydrogen blocks the reaction site for intramolecular hydrogen shift reaction same as the case of Rh cluster complexes. Fig. 9(b) represents the isotopic distribution in the reaction of propene-1-d_1 in the presence of H_2, confirming the 1,3- and 2,3-intramolecular hydrogen exchange process.

3.4. C_3H_6–C_3D_6 and C_3H_6–D_2 reactions over Rh/Al_2O_3 and Ru/Al_2O_3 catalysts

To compare the catalytic difference between carbonyl cluster complexes and metal surfaces, $Rh_4(CO)_{12}/Al_2O_3$ and $Ru_3(CO)_{12}/Al_2O_3$ were reduced by hydrogen at 723 K for 20 h, and C_3H_6–C_3D_6 and C_3H_6–D_2 reactions were studied. The results of the temperature dependencies were summarized in Figs. 4 and 7. In the case of C_3H_6–D_2 reaction over Rh/SiO_2 (Fig. 4), the TOF for propane and monodeuteropropene formations became much larger than the case of $Rh_4(CO)_{12}/Al_2O_3$ complexes with higher activation energies (E = 43.1 kJ/mol both). On the contrary, the TOF of C_3H_6–C_3D_6 reaction over Rh/Al_2O_3 was much smaller than that of C_3H_6–D_2 reaction with still higher activation energy (E = 76.9 kJ/mol), which was completely opposite from the case of Rh carbonyl cluster complexes.

The microwave spectroscopic results of the monodeuteropropene formed during C_3H_6–D_2 reaction over Rh/Al_2O_3 are shown in Fig. 10(a) over reduced surface, and in Fig. 10(b) over CO preadsorbed surface. Over reduced surface the main products were c- and t-propene-1-d_1(37% each) with a small amount of propene-2-d_1(17%) and propene-3-d_1(8%). Because C_3H_6–C_3D_6

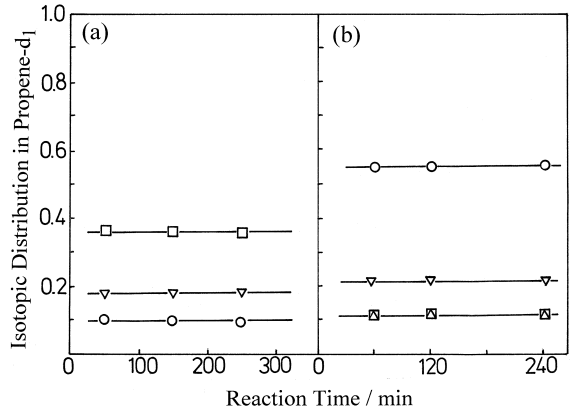

Fig. 10. Time courses of the isotopic distribution in propene-d_1 during C_3H_6–D_2 reaction over (a) freshly reduced Rh/Al_2O_3 at 180 K and (b) CO preadsorbed Rh/Al_2O_3 at 273 K. P(propene) = 15 Torr, and $P(D_2)$ = 30 Torr. 0.5 g of catalyst. □, c-1-d_1; △, t-1-d_1; ▽, 2-d_1; ○, 3-d_1.

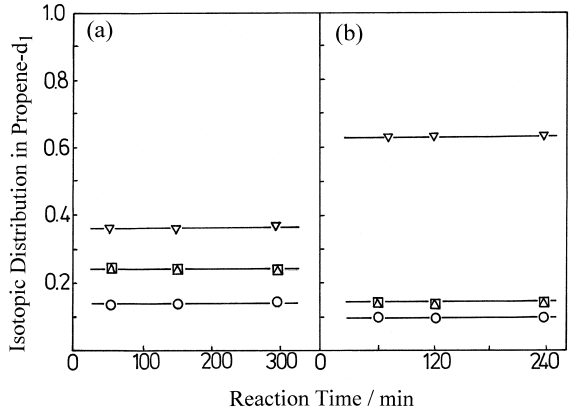

Fig. 11. Time courses of the isotopic distribution in propene-d_1 during C_3H_6–D_2 reaction over (a) freshly reduced Ru/Al_2O_3 at 180 K and (b) CO preadsorbed Rh/Al_2O_3 at 298 K. P(propene) = 15 Torr, and $P(D_2)$ = 30 Torr. 0.5 g of catalyst. □, *c*-1-d_1; △, *t*-1-d_1; ▽, 2-d_1; ○, 3-d_1.

exchange (dissociative mechanism) is more than three orders of magnitudes slower, this reaction should proceed by the associative mechanism through *n*-propyl and sec-propyl adsorbed intermediates. But the ratio of formed propene-3-d_1 to propene-1-d_1 is much smaller than the theoretical value (3:2), which indicates that adsorbed state of sec-propyl species is sterically distorted. When CO was preadsorbed on this surface, the distribution pattern changed considerably as shown in Fig. 10(b), which is remarkably different from Fig. 10(a).

Similar results in temperature dependencies were obtained over Ru/Al_2O_3 catalysts as shown in Fig. 7. C_3H_6–D_2 reaction was much faster than C_3H_6–C_3D_6 reaction, which is quite different from Ru carbonyl cluster complexes. The isotopic distribution patterns of monodeuteropropene formed in C_3H_6–D_2 reaction is shown in Fig. 11(a), together with that of CO preadsorbed surface in Fig. 11(b). Again remarkably different distribution patterns were observed for each other.

4. Discussion

As mentioned already microwave spectroscopy is a powerful technique for the study of hydrogen exchange of propene, which enables us to determine the previous points of attachment of the adsorbed molecules to the catalysts by analyzing the distribution of the D atoms in the exchanged d_1-molecule. The most common mechanism for hydrogen exchange in C_3H_6–C_3D_6 reaction is the dissociative one as shown in Scheme 1(a). If we take this mechanism to explain the isotopic distribution pattern obtained in Fig. 2(a), the dissociation of hydrogen takes place only at the double bond carbons of propene molecule forming *n*-propenyl and sec-propenyl adsorbed species.

The other possible mechanism involves surface hydrides as shown in Scheme 1(c). It is well known that such hydride is formed by the reaction with surface OH groups in the case of Os and Ru carbonyl cluster complexes [16,17]. Remarkably high TOF and low activation energy in C_3H_6–C_3D_6 reaction over fixed cluster complexes may well be explained by this hydride mechanism. Moreover, the coincidence of the TOFs and activation energies between H_2–D_2 exchange and C_3H_6–C_3D_6 exchange reactions over $Rh_4(CO)_{12}/Al_2O_3$ complexes is also understandable if we assume the same rate determining step of metal-hydride bond scission process after the formation of activated complexes between a metal-hydride and a hydrogen molecule or a propene molecule.

On the other hand, the rate of the exchange process in the C_3H_6–D_2 reaction was one to two orders of magnitude slower than that of C_3H_6–C_3D_6 or H_2–D_2 reaction. The rate of H_2–D_2 exchange in the presence of propene was also plotted in Fig. 4, which is similar to the exchange process in C_3H_6–D_2 reaction. These results strongly suggest that the rate determining step in C_3H_6–D_2 reaction is the dissociation of deuterium molecules, which is strongly retarded by the adsorbed propene molecules. And once deuterium atom is formed it is incorporated into the propene molecules through the dissociatively adsorbed intermediates. This is the reason why the isotopic distribution in formed monodeuteropropene in C_3H_6–D_2 reaction are in equilibrium.

The trend is quite different over supported metal catalysts, where C_3H_6–D_2 reaction was much faster than C_3H_6–C_3D_6 reaction as summarized in Figs. 4 and 7. Since the inhibition of adsorbed propene for the dissociation of deuterium molecule is not so strong over reduced metal catalysts compared to the cases of carbonyl metal cluster complexes, deuterium addition and exchange reactions take place with much faster rates than those over cluster catalysts. On the contrary, deuterium exchange in C_3H_6–C_3D_6 reaction over reduced metal catalysts was much slower than that over fixed carbonyl metal cluster complexes. This is probably because of the requirement of higher temperatures for the dissociation of C–H bond or higher stability of dissociatively adsorbed propene in the case of reduced metal catalysts. When CO was preadsorbed on the reduced Rh metal catalyst, the rate of C_3H_6–D_2 reaction decreased in more than three orders of magnitudes, which is also much slower than C_3H_6–D_2 reaction over $Rh_4(CO)_{12}/Al_2O_3$ catalyst. It is also quite interesting that the structure of the reaction intermediates changes significantly by the presence of preadsorbed CO over Rh and Ru metal catalysts as shown in Figs. 10 and 11. These phenomena may be explained by the geometric as well as the electronic effects of adsorbed CO.

Among fixed group VIII metal carbonyl cluster complexes, alumina-supported triosmium and tetrairidium carbonyl cluster complexes are the most thoroughly studied catalytic system by B.C. Gates et al. In the cases of hexene-1 isomerization over $Os_3(CO)_{12}/Al_2O_3$ [18,19], but-1-ene isomerization over $Os_4(CO)_{12}/Al_2O_3$ [20] and toluene hydrogenation over $Ir_4(CO)_{12}/Al_2O_3$ [21], surface bound hydride complexes formed by the oxidative addition reaction of the cluster complex with surface –OH groups are proposed to be the catalytically active species. They proposed an insertion mechanism involving hydride ligands on the osmium or iridium, which seems to be similar to the Scheme 1(c) in our study. The breakup of the metal–metal bond in the cluster complexes takes place at higher temperatures, giving surface-bound mononuclear Os(II) or Ir(II) complexes having 2 or 3 CO ligands.

In the cases of fixed Rh and Ru carbonyl cluster complexes, this breakup of the cluster structure seems to take place during the impregnation procedure at room temperature and resulting $[M(CO)_2]_n$ surface ensembles are very active in propene–deuterium exchange reaction. As mentioned already its catalytic behavior is completely different from that of reduced metal catalysts, indicating that the electronic state of these surface ensembles is positively charged same as the case of Os and Ir clusters. In spite of the different nuclearity of the cluster and even different kind of metals, similar catalytic activity and similar structure of reaction intermediates are observed in C_3H_6–C_3D_6 exchange reaction, which may be explained by the presence of the common catalytic active species such as surface hydride similar to the Os and Ir clusters, although they are not detected in these systems.

References

[1] A. Theolier, A.K. Smith, M. Leconte, J.M. Basset, G.M. Zanderighi, R. Psaro, R. Ugo, J. Organomet. Chem. 191 (1980) 415.
[2] A.K. Smith, F. Hugues, A. Theolier, J.M. Basset, R. Ugo, M. Zanderighi, J.L. Bilhou, V. Bilhou-Bougnol, W.F. Graydon, Inorg. Chem. 18 (1979) 3104.
[3] V. Adimir, L. Kuznetsov, A.T. Bell, Y.I. Yermakov, J. Catal. 65 (1980) 374.
[4] A. Zecchina, E. Guglielminotti, A. Bossi, M. Camia, J. Catal. 74 (1982) 225.
[5] Z. Schay, K. Lazar, J. Mink, L. Guczi, J. Catal. 87 (1984) 179.
[6] A.K. Smith, A. Theolier, J.M. Basset, R. Ugo, D. Commereuc, Y. Chauvin, J. Am. Chem. Soc. 100 (1978) 2590.
[7] A. Brenner, D.A. Hucul, J. Am. Chem. Soc. 102 (1980) 2484.
[8] S. Uchiyama, B.C. Gates, J. Catal. 110 (1988) 388.
[9] S. Kondo, S. Saito, K. Tamaru, J. Am. Chem. Soc. 96 (1974) 6857.
[10] S. Naito, M. Tanimoto, J. Catal. 102 (1986) 377.
[11] S. Naito, M. Tanimoto, J. Chem. Soc., Faraday Trans. 1 83 (1987) 2475.

[12] S. Naito, M. Tanimoto, J. Chem. Soc., Faraday Trans. 1 84 (1988) 4115.
[13] S. Naito, M. Tanimoto, J. Catal. 119 (1989) 300.
[14] S. Naito, M. Tanimoto, Bull. Chem. Soc. Jpn. 67 (1994) 3211.
[15] W.P. Norris, J. Org. Chem. 24 (1959) 1579.
[16] M. Deeba, B.C. Gates, J. Catal. 67 (1981) 303.
[17] V.L. Kuzunetsov, A.T. Bell, Y.I. Yermakov, J. Catal. 65 (1980) 374.
[18] X.-J. Li, B.C. Gates, J. Catal. 84 (1983) 55.
[19] X.-J. Li, J.H. Onuferko, B.C. Gates, J. Catal. 85 (1984) 176.
[20] T.R. Krause, M.E. Davies, J. Lieto, B.C. Gates, J. Catal. 94 (1985) 195.
[21] A. Zhao, B.C. Gates, J. Catal. 168 (1997) 60.